T-Circuit Model of Asynchronous Wind Turbine for Distribution System Load Flow Analysis

Rudy Gianto*, [1]

www.rericjournal.ait.ac.th

Abstract – *It is widely acknowledged that for modern electric distribution system embedded with wind turbine generators, the conventional load flow analysis needs to be reformulated to include the wind turbine generating system (WTGS) model in the analysis. This paper presents a simple method for modeling and incorporating fixed-speed WTGS into distribution system load flow analysis. The proposed model for the WTGS is developed based on the equivalent T-circuit of the asynchronous machine of the WTGS where only Kirchhoff and Ohm laws are used in forming the mathematical model. Unlike the previous model (i.e. PQ model), conversion from T-circuit to π-circuit is not necessary in the proposed model development. Moreover, since only one set of equations is needed to represent the WTGS, the proposed T-circuit model is therefore much simpler than the PQ model. The model is then integrated into the load flow algorithm to evaluate steady state operation of the distribution system and the WTGS. Test results on 33-node and 69-node distribution networks indicate that the proposed method is accurate and valid.*

Keywords – *asynchronous generator, distribution system, induction generator, load flow analysis, wind turbine.*

1. INTRODUCTION

Recently, integration of wind turbine generating system (WTGS) into power grid has significantly increased. For the last ten years, the yearly average growth of wind turbine has increased by 30% world-wide. At the end of 2015, the total installed capacity of wind turbine is around 433 GW. It is expected that at the end of 2030, the capacity can be increased to 2110 GW which will cover 20% of the world electricity demand.

However, it has been known that WTGS integration into power grid (power or distribution system) can cause some problems. These problems come from the natural behaviours of the wind energy itself which are unpredicted and fluctuated. In turn, these problems will affect system performances of the power grid in terms of its steady-state and dynamic operations.

It has generally been accepted that load flow analysis is the most widely used tool for determining the steady-state operation of an electric power system. It is also acknowledged that for modern power system containing WTGS, the conventional load flow problem needs to be reformulated to include the WTGS mathematical model. Many investigations have been carried out, and several interesting methods have been proposed for modeling and incorporating the WTGS into load flow analysis [1]-[9].

In [1], mathematical representation of WTGS and its inclusion in the load flow solution approach has been addressed. The approach proposed in [1] uses a set of nonlinear equations obtained from active- and reactive-power balance at all nodes of the power system including the WTGS nodes. The Newton-Raphson

method is then used to find a solution to the set of equations. In references [2]-[4], mathematical model of asynchronous wind turbine for power system steady state analysis has been proposed. The model in references [2]-[4] is based on the equations that calculate active- and reactive-power exchanged between the asynchronous machine and the electric power network.

In reference [5], the WTGS is assumed to have specified values of real- and reactive-power outputs. It is therefore can be treated as PQ node in the load flow analysis. The Newton-Raphson technique is then employed as a load flow solution method. Reference [6] develops a WTGS model to be used in balanced or unbalanced distribution system load flow analysis. The developed mathematical model is expressed in the forms of WTGS output power where it has been formulated as a function of induction generator parameters, terminal voltage and turbine mechanical power.

References [7]-[9] propose a unique technique to integrate fixed-speed WTGS into load flow analysis. The method adds two internal nodes into the existing (original) power network. These internal nodes are required to represent the electrical circuits of WTGS asynchronous machine and wind turbine mechanical power. The internal nodes are treated as conventional PQ nodes, and standard load flow program can then be used in the analysis.

In the present paper, a simple method for modeling and incorporating WTGS into distribution system load flow analysis is proposed. The proposed model is developed based on the equivalent T-circuit of the WTGS asynchronous machine. It is derived using basic electric circuit theory, where only Kirchhoff and Ohm laws are used in forming the mathematical model. Unlike the previous model (*i.e.* PQ model), conversion from T-circuit to π-circuit is not necessary in the model derivation process. Moreover, since only one set of equations is needed to represent the WTGS, it is therefore much simpler than the PQ model. The

---

* Department of Electrical Engineering, University of Tanjungpura, Indonesia.

[1] Corresponding author;
E-mail: rudy.gianto@ee.untan.ac.id.

proposed model can easily be integrated into the power or distribution system load flow analysis.

The content of the present paper is organized as follows: Section 2 addresses the distribution system load flow analysis. Formulation of traditional load flow problem is discussed in this section. Section 3 describes the proposed WTGS model and its integration into distribution system load flow analysis. Solution technique for the load flow problem using Newton-Raphson method is briefly discussed in Section 4. Study cases are given in Section 5 where verification and validation of the proposed method are also presented. Finally, Section 6 points out the conclusions of the present work.

2. DISTRIBUTION LOAD FLOW ANALYSIS

Load flow (or power flow) is probably one of the important analyses in electric power system study. Load flow analysis is carried out to determine the electrical quantities such as: bus (nodal) voltages, power generations, line power flows and losses. By knowing the above electrical quantities, steady-state operation of a power system (or distribution system) can then be assessed and evaluated.

For system without wind turbine generator, solution to the load flow problem is usually obtained by solving the following nonlinear equations:

$$S_{Gi} - S_{Li} - V_i \sum_{j=1}^{n} Y_{ij}^* V_j^* = 0 \qquad (1)$$

where:

n	: total number of buses (nodes)
i = 1, 2, …, n	: bus number
$S_{Gi} = P_{Gi} + jQ_{Gi}$	: power generation at bus i
$S_{Li} = P_{Li} + jQ_{Li}$	: power load at bus i
$V_i = |V_i|e^{j\delta i}$	: voltage at bus i
$Y_{ij} = |Y_{ij}|e^{j\delta ij}$	: element ij of admittance matrix

Equation 1 shows that each bus in the system is characterized by four variables: P_{Gi}, Q_{Gi}, $|V_i|$, and δ_i. To make the equation solvable, it is common in distribution system load flow analysis to define two types of buses as shown in Table 1. By using the definition, solution to equation 1 can then be found since the number of unknowns is now equal to the number of equations (each bus has two unknowns and two equations). It is to be noted that voltage at substation bus is generally specified at a certain value (it is usually assumed to be $1.0 \angle 0°$ pu).

Table 1. Bus types and quantities.

Bus Type	Known Quantity	Unkown Quantity
Substation	$|V|=1.0$ and $\delta = 0$	P_G and Q_G
Load	$P_G = Q_G = 0$	$|V|$ and δ

Equation 1 is the formulation of load flow problem for system without wind turbine generator. However, for modern system embedded with wind turbine generator, additional equation is needed to complete the formulation of the load flow problem. Derivation of wind turbine generator mathematical model and its integration into load flow analysis is discussed in the following section.

3. PROPOSED WTGS MODEL

A fixed-speed WTGS with SCIG (Squirrel Cage Induction Generator) as the energy converter is shown Figure 1(a). It can be seen from the figure that the WTGS is connected to bus k of an electric distribution system. Whereas, Figure 1(b) shows the SCIG input and output powers, where P_m and S_g represent mechanical power input and electrical power output of the SCIG, respectively. It is to be noted that P_m is also power delivered by the wind turbine, and it can be determined using the power curve provided by the turbine manufacture.

(a)

(b)
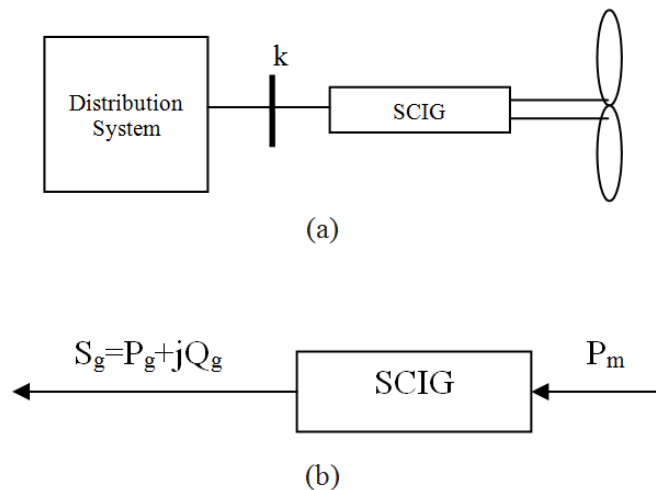
Fig. 1. WTGS connected to distribution system.

Equivalent circuit of the SCIG is shown in Figure 2, where R_1, X_1, R_2, X_2, R_c, X_m and $R_2(1-s)/s$ denote stator resistance, stator leakage reactance, rotor resistance, rotor leakage reactance, core loss resistance, magnetic reactance, and dynamic resistance, respectively. It is also to be noted that power dissipated in the dynamic resistance represents the mechanical power P_m.
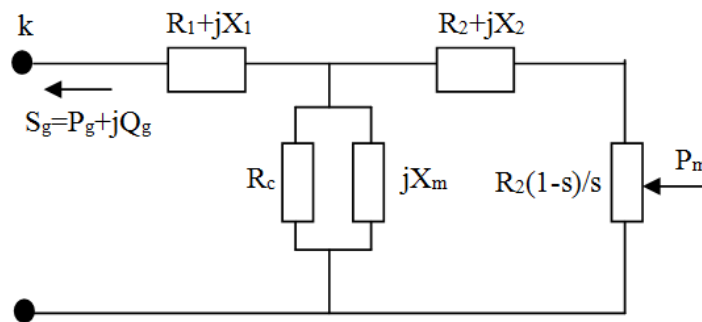
Fig. 2. Steady-state equivalent circuit of SCIG.
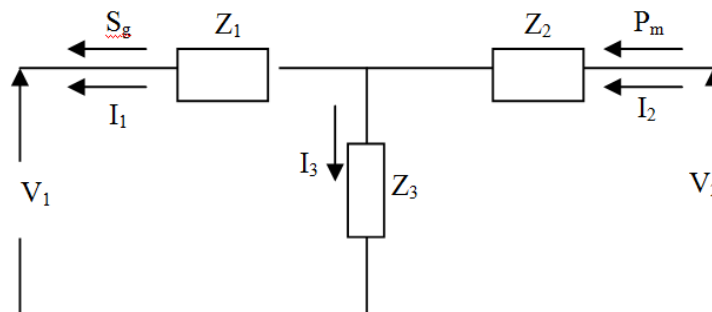
Fig. 3. Equivalent circuit of SCIG in terms of impedances.

Modeling and integration of the WTGS into load flow analysis is explained in the following. The development of the proposed SCIG mathematical model will be based on electric circuit theory, where Kirchhoff and Ohm laws are used in forming the model.

Figure 3 shows the equivalent circuit of SCIG in terms of impedances Z_1, Z_2 and Z_3. Based on Figures 2 and 3, the impedances of Z_1, Z_2 and Z_3 can be formulated as:

$$Z_1 = R_1 + jX_1$$
$$Z_2 = R_2 + jX_2 \qquad (2)$$
$$Z_3 = jR_cX_m /(R_c + jX_m)$$

Quantities V_1, I_1, V_2, I_2, and I_3 in Figure 3 denote the stator voltage, stator current, rotor voltage, rotor current, and magnetic circuit current, respectively. Based on Figure 3, the WTGS electrical power output is calculated as the following:

$$S_g = P_g + jQ_g = V_1I_1 * \qquad (3)$$

and the WTGS mechanical power input can also be formulated as:

$$S_m = P_m = V_2I_2 * \qquad (4)$$

Furthermore, from Figure 3, the rotor voltage is given by:

$$V_2 = V_1 + I_1Z_1 + I_2Z_2 \qquad (5)$$

Whereas, the rotor and magnetic circuit currents can be written as:

$$I_2 = I_1 + I_3 \qquad (6)$$

and:

$$I_3 = \frac{V_1 + I_1Z_1}{Z_3} \qquad (7)$$

Substituting Equation 7 into Equation 6, the rotor current becomes:

$$I_2 = V_1\frac{1}{Z_3} + I_1\frac{Z_1 + Z_3}{Z_3} \qquad (8)$$

On using Equation 8 in Equation 5, the rotor voltage can be rewritten as:

$$V_2 = V_1\left(1 + \frac{Z_2}{Z_3}\right) + I_1\left(Z_1 + Z_2 + \frac{Z_1Z_2}{Z_3}\right) \qquad (9)$$

Substituting Equations 9 and 8 into Equation 4, and rearranging, the WTGS mechanical power becomes:

$$S_m = V_1V_1 * Z_{T1} + V_1I_1 * Z_{T2} + V_1 * I_1Z_{T3} + I_1I_1 * Z_{T4} \qquad (10)$$

where:

$$Z_{T1} = \frac{1}{Z_3*} + \frac{Z_2}{Z_3 Z_3*}$$

$$Z_{T2} = 1 + \frac{Z_1*}{Z_3*} + \frac{Z_2}{Z_3} + \frac{Z_1*Z_2}{Z_3 Z_3*}$$

$$Z_{T3} = \frac{Z_1}{Z_3*} + \frac{Z_1 Z_2}{Z_3 Z_3*} + \frac{Z_2}{Z_3*}$$
(11)

$$Z_{T4} = Z_1 + Z_2 + \frac{Z_1 Z_1*}{Z_3*} + \frac{Z_1 Z_2}{Z_3} + \frac{Z_1 Z_1*Z_2}{Z_3 Z_3*} + \frac{Z_1*Z_2}{Z_3*}$$

On using Equation 3 in Equation 10, the expression for WTGS mechanical power can be formulated as the following:

$$S_m = V_1 V_1 * Z_{T1} + S_g Z_{T2} + S_g * Z_{T3} + \frac{S_g S_g *}{V_1 V_1 *} Z_{T4} \quad (12)$$

Equation 12 is the proposed mathematical model of fixed-speed WTGS to be incorporated into the distribution system load flow analysis. It is to be noted that V_1 in Equation 12 is also the voltage at the WTGS bus. Therefore, to obtain the load flow solution for modern system with WTGS, the equations to be solved simultaneously are Equations 1 and 12. Table 2 shows the known and unknown quantities in the complete formulation of load flow problem for system with WTGS.

Table 2. Bus types and quantities for system with WTGS.

Bus Type	Known Quantity	Unnown Quantity
Substation	$\|V\|=1.0$ and $\delta = 0$	P_G and Q_G
Load	$P_G=Q_G= 0$	$\|V\|$ and δ
WTGS	$P_G=Q_G= 0$	P_g, Q_g, $\|V\|$ and δ

4. SOLUTION TECHNIQUE

It has been discussed in Section 3 that in load flow analysis, the equations to be solved are nonlinear. A solution to this set of nonlinear equations is usually obtained by iterative approach (for example: Newton-Raphson method). In the method, the first step in the calculation process is to estimate the initial values for the solution (unknown quantities). This initial estimation is then iteratively improved until the solution with desired accuracy is found.

The following is brief explanation of Newton-Raphson method in finding the solution to general set of equations. Suppose the nonlinear equations to be solved are arranged in the form of vector function as follows:

$$\mathbf{F(x)} = \begin{bmatrix} f_1(x_1, x_2, ..., x_n) \\ f_2(x_1, x_2, ..., x_n) \\ \vdots \\ f_n(x_1, x_2, ..., x_n) \end{bmatrix} = \mathbf{0} \quad (13)$$

Then, the search for the solution is carried out by using the following equation:

$$\mathbf{x}^{(k+1)} = \mathbf{x}^{(k)} + \mathbf{d}^{(k)} \quad (14)$$

where k is the iteration count, **x** is the vector of solution, and **d** is the vector of correction factors.

It is to be noted that in Equation 14, **x** is usually calculated repeatedly to obtain an accurate solution. Vector of correction factors **d** can be determined by solving the following set of linear equations:

$$\mathbf{J(x}^{(k)})\mathbf{d}^{(k)} = -\mathbf{F(x}^{(k)}) \quad (15)$$

where $\mathbf{J(x)}$ is Jacobian matrix of $\mathbf{F(x)}$. Elements of the Jacobian matrix are computed using partial derivatives and the formulation is given by:

$$\mathbf{J(x)} = \begin{bmatrix} \frac{\partial f_1}{\partial x_1} & \frac{\partial f_1}{\partial x_2} & \cdots & \frac{\partial f_1}{\partial x_n} \\ \frac{\partial f_2}{\partial x_1} & \frac{\partial f_2}{\partial x_2} & \cdots & \frac{\partial f_2}{\partial x_n} \\ \vdots & \vdots & \ddots & \vdots \\ \frac{\partial f_n}{\partial x_1} & \frac{\partial f_n}{\partial x_2} & \cdots & \frac{\partial f_n}{\partial x_n} \end{bmatrix} \quad (16)$$

The elements of Jacobian matrix can be obtained analytically or numerically. However, the application of numerical method is more common as it is easier and more efficient. Determination of Jacobian matrix using numerical method is explained in the Appendix.

5. RESULTS AND DISCUSSION

5.1 Test System

Verification of the proposed T-circuit model of WTGS for load flow analysis is carried out by using the following two test systems:

(i)   33-bus distribution network

Single line diagram of the network is shown in Figure 4 [10]. It can be seen from the figure that the distribution system comprises of 33 buses and 32 lines (branches). It has the system voltage of 12,66 kV and total connected load of 3715 kW and 2300 kVAR. Details of the system data are presented in Table 3.

(ii)   69-bus distribution network

Figure 5 shows diagram of the network [10]. It can be observed from the figure that the distribution system comprises of 69 buses and 68 lines (branches). Also, it has the system voltage of 12,66 kV and total connected load of 3801.890 kW and 2694.100 kVAR. Details of the system data are given in Table 4.

Table 3. 33-bus system data.

Line No	Send Bus	Rec. Bus	R* (ohm)	X* (ohm)	PL** (KW)	QL** (KVAR)
1	1	2	0.0922	0.0470	100	60
2	2	3	0.4930	0.2511	90	40
3	3	4	0.3660	0.1864	120	80
4	4	5	0.3811	0.1941	60	30
5	5	6	0.8190	0.7070	60	20
6	6	7	0.1872	0.6188	200	100
7	7	8	1.7114	1.2351	200	100
8	8	9	1.0300	0.7400	60	20
9	9	10	1.0440	0.7400	60	20
10	10	11	0.1966	0.0650	45	30
11	11	12	0.3744	0.1238	60	35
12	12	13	1.4680	1.1550	60	35
13	13	14	0.5416	0.7129	120	80
14	14	15	0.5910	0.5260	60	10
15	15	16	0.7463	0.5450	60	20
16	16	17	1.2890	1.7210	60	20
17	17	18	0.7320	0.5740	90	40
18	2	19	0.1640	0.1565	90	40
19	19	20	1.5042	1.3554	90	40
20	20	21	0.4095	0.4784	90	40
21	21	22	0.7089	0.9373	90	40
22	3	23	0.4512	0.3083	90	50
23	23	24	0.8980	0.7091	420	200
24	24	25	0.8960	0.7011	420	200
25	6	26	0.2030	0.1034	60	25
26	26	27	0.2842	0.1447	60	25
27	27	28	1.0590	0.9337	60	20
28	28	29	0.8042	0.7006	120	70
29	29	30	0.5075	0.2585	200	600
30	30	31	0.9744	0.9630	150	70
31	31	32	0.3105	0.3619	210	100
32	32	33	0.3410	0.5302	60	40

* Each value of impedance should be divided by 12.66^2
**Load connected to receiving bus
**Each value of load should be divided by 1000
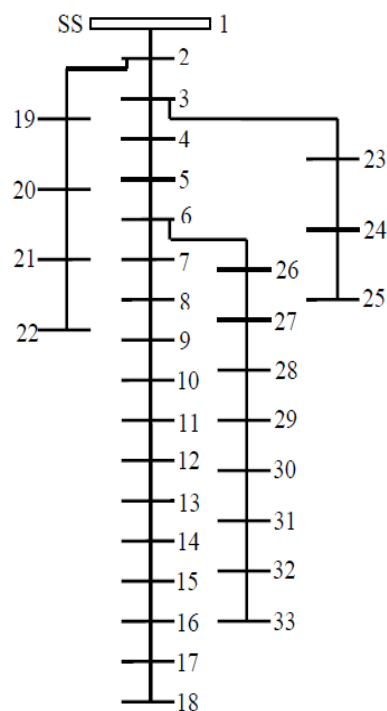
Fig. 4. 33-bus distribution network.

Table 4. 69-bus system data.

Line No	Send Bus	Rec. Bus	R* (ohm)	X*(ohm)	PL** (KW)	QL** (KVAR)
1	1	2	0.0005	0.0012	0	0
2	2	3	0.0005	0.0012	0	0
3	3	4	0.0015	0.0036	0	0
4	4	5	0.0251	0.0294	0	0
5	5	6	0.3660	0.1864	2.6	2.2
6	6	7	0.3810	0.1941	40.4	30
7	7	8	0.0922	0.0470	75	54
8	8	9	0.0493	0.0251	30	22
9	9	10	0.8190	0.2707	28	19
10	10	11	0.1872	0.0619	145	104
11	11	12	0.7114	0.2351	145	104
12	12	13	1.0300	0.3400	8	5
13	13	14	1.0440	0.3450	8	5.5
14	14	15	1.0580	0.3496	0	0
15	15	16	0.1966	0.0650	45.5	30
16	16	17	0.3744	0.1238	60	35
17	17	18	0.0047	0.0016	60	35
18	18	19	0.3276	0.1083	0	0
19	19	20	0.2106	0.0690	1	0.6
20	20	21	0.3416	0.1129	114	81
21	21	22	0.0140	0.0046	5	3.5
22	22	23	0.1591	0.0526	0	0
23	23	24	0.3463	0.1145	28	20
24	24	25	0.7488	0.2475	0	0
25	25	26	0.3089	0.1021	14	10
26	26	27	0.1732	0.0572	14	10
27	3	28	0.0044	0.0108	26	18.6
28	28	29	0.0640	0.1565	26	18.6
29	29	30	0.3978	0.1315	0	0
30	30	31	0.0702	0.0232	0	0
31	31	32	0.3510	0.1160	0	0
32	32	33	0.8390	0.2816	14	10
33	33	34	1.7080	0.5646	19.5	14
34	34	35	1.4740	0.4873	6	4
35	3	36	0.0044	0.0108	26	18.55
36	36	37	0.0640	0.1565	26	18.55
37	37	38	0.1053	0.1230	0	0
38	38	39	0.0304	0.0355	24	17
39	39	40	0.0018	0.0021	24	17
40	40	41	0.7283	0.8509	1.2	1
41	41	42	0.3100	0.3623	0	0
42	42	43	0.0410	0.0478	6	4.3
43	43	44	0.0092	0.0116	0	0
44	44	45	0.1089	0.1373	39.22	26.3
45	45	46	0.0009	0.0012	39.22	26.3
46	4	47	0.0034	0.0084	0	0
47	47	48	0.0851	0.2083	79	56.4
48	48	49	0.2898	0.7091	384.7	274.5
49	49	50	0.0822	0.2011	384.7	274.5
50	8	51	0.0928	0.0473	40.5	28.3
51	51	52	0.3319	0.1114	3.6	2.7
52	9	53	0.1740	0.0886	4.35	3.5
53	53	54	0.2030	0.1034	26.4	19
54	54	55	0.2842	0.1447	24	17.2
55	55	56	0.2813	0.1433	0	0
56	56	57	1.5900	0.5337	0	0
57	57	58	0.7837	0.2630	0	0
58	58	59	0.3042	0.1006	100	72
59	59	60	0.3861	0.1172	0	0
60	60	61	0.5075	0.2585	1244	888

61	61	62	0.0974	0.0496	32	23
62	62	63	0.1450	0.0738	0	0
63	63	64	0.7105	0.3619	227	162
64	64	65	1.0410	0.5302	59	42
65	11	66	0.2012	0.0611	18	13
66	66	67	0.0047	0.0014	18	13
67	12	68	0.7394	0.2444	28	20
68	68	69	0.0047	0.0016	28	20

* Each value of impedance should be divided by 12.66^2

**Load connected to receiving bus

**Each value of load should be divided by 1000
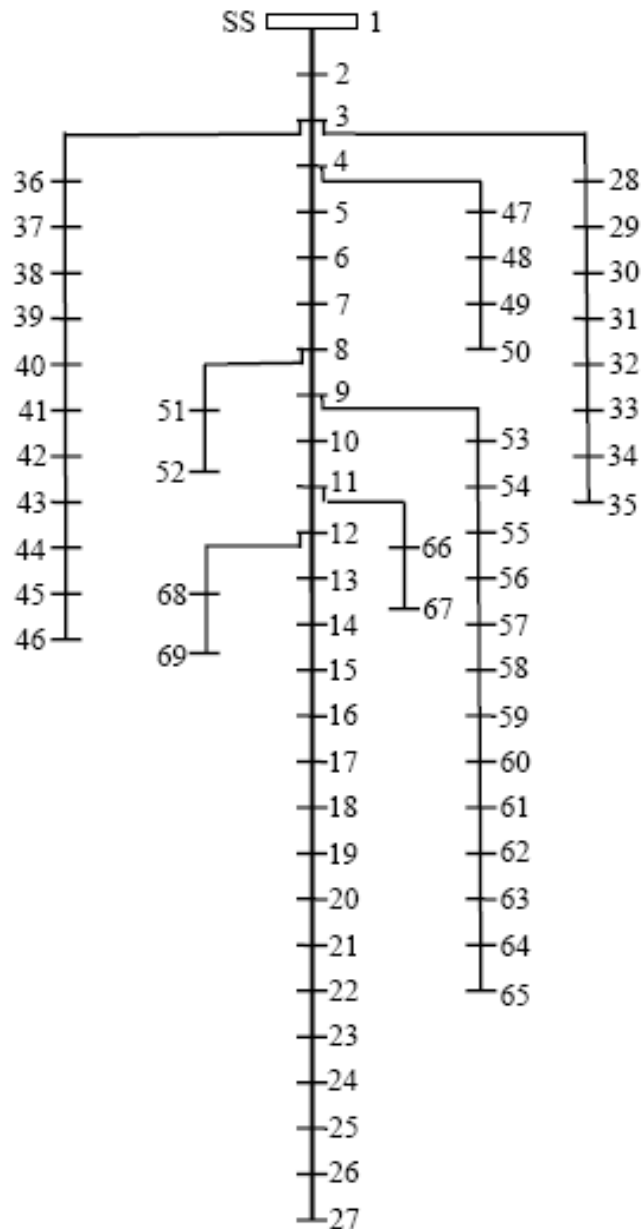
Fig. 5. 69-bus distribution network.

Details data of the WTGS used in the validation study are shown in Table 5. It is to be noted that all data (WTGS and distribution system data) are in pu on 1 MVA base. Also, for 33-bus network, the WTGS is assumed to be connected to bus 33, whereas, for 69-bus network, the WTGS is connected to bus 69.

Table 5. SCIG of WTGS data.

Parameter	R1	X1	R2	X2	Rc	Xm
Value	0.01	0.05	0.01	0.05	100	5

5.2 Discussion

Results of the load flow calculations are shown in Tables 6 to 8. Table 6 shows the calculated voltage magnitudes at WTGS buses, and Tables 7 and 8 show the calculated WTGS electrical power outputs. It is to be noted that the calculations are carried out for various values of mechanical powers (P_m) ranging from 0.1 to 1.0 pu. These values represent the low speed to higher speed wind conditions.

For comparison purposes, results from other method as proposed by researches [2]-[4] are also presented in Tables 6 to 8. It can be seen that the results of the proposed method are accurate and in exact agreement with the PQ model method [2]-[4]. These comparisons confirm that the proposed T-circuit model is valid and therefore can be used for incorporating fixed-speed WTGS into distribution load flow analysis.

As fixed-speed WTGS is usually equipped with capacitor to compensate the reactive-power consumed by the induction generator, investigation on the effects of the capacitor installation at WTGS terminal are also presented in this paper. It is assumed that the capacitor capacity is 0.5 pu. Tables 9 and 10 show the WTGS voltage magnitudes and power generations with the capacitor installed in the systems.

Table 6. Voltage magnitude at WTGS bus.

Pm	Proposed Method		PQ Model	
	33-bus	69-bus	33-bus	69-bus
0.1	0.91419	0.96823	0.91419	0.96823
0.2	0.91866	0.97038	0.91866	0.97038
0.3	0.92296	0.97249	0.92296	0.97249
0.4	0.92710	0.97457	0.92710	0.97457
0.5	0.93108	0.97661	0.93108	0.97661
0.6	0.93492	0.97861	0.93492	0.97861
0.7	0.93861	0.98058	0.93861	0.98058
0.8	0.94217	0.98252	0.94217	0.98252
0.9	0.94559	0.98442	0.94559	0.98442
1.0	0.94888	0.98630	0.94888	0.98630

Table 7. WTGS electric power generation (33-bus).

Pm	Proposed Method	PQ Model
0.1	0.0912-j0.1670	0.0912-j0.1670
0.2	0.1904-j0.1724	0.1904-j0.1724
0.3	0.2892-j0.1801	0.2892-j0.1801
0.4	0.3875-j0.1899	0.3875-j0.1899
0.5	0.4854-j0.2018	0.4854-j0.2018
0.6	0.5828-j0.2157	0.5828-j0.2157
0.7	0.6799-j0.2315	0.6799-j0.2315
0.8	0.7765-j0.2493	0.7765-j0.2493
0.9	0.8728-j0.2689	0.8728-j0.2689
1.0	0.9687-j0.2904	0.9687-j0.2904

Table 8. WTGS electric power generation (69-bus).

Pm	Proposed Method	PQ Model
0.1	0.0902-j0.1870	0.0902-j0.1870
0.2	0.1895-j0.1913	0.1895-j0.1913
0.3	0.2884-j0.1977	0.2884-j0.1977
0.4	0.3869-j0.2061	0.3869-j0.2061
0.5	0.4850-j0.2164	0.4850-j0.2164
0.6	0.5827-j0.2287	0.5827-j0.2287
0.7	0.6800-j0.2430	0.6800-j0.2430
0.8	0.7769-j0.2590	0.7769-j0.2590
0.9	0.8734-j0.2770	0.8734-j0.2770
1.0	0.9696-j0.2968	0.9696-j0.2968

Table 9. Voltage magnitude at WTGS bus and WTGS power generation with capacitor installed (33-bus).

Pm	Voltage Magnitude	WTGS Power
0.1	0.93305	0.0909-j0.1738
0.2	0.93744	0.1901-j0.1792
0.3	0.94167	0.2889-j0.1866
0.4	0.94575	0.3873-j0.1961
0.5	0.94968	0.4852-j0.2076
0.6	0.95348	0.5828-j0.2211
0.7	0.95715	0.6799-j0.2364
0.8	0.96069	0.7767-j0.2536
0.9	0.96411	0.8731-j0.2726
1.0	0.96740	0.9692-j0.2934

Table 10. Voltage magnitude at WTGS bus and WTGS power generation with capacitor installed (69-bus).

Pm	Voltage Magnitude	WTGS Power
0.1	0.97250	0.0901-j0.1886
0.2	0.97464	0.1895-j0.1929
0.3	0.97675	0.2884-j0.1992
0.4	0.97882	0.3869-j0.2076
0.5	0.98085	0.4850-j0.2179
0.6	0.98285	0.5827-j0.2301
0.7	0.98482	0.6800-j0.2442
0.8	0.98675	0.7769-j0.2601
0.9	0.98866	0.8735-j0.2780
1.0	0.99053	0.9697-j0.2976

Variation of WTGS terminal voltage and power generation output against mechanical power input are also depicted in Figures 6 to 11. As expected, installation of the capacitor improves the profile of WTGS terminal voltage (see Figures 6 and 7). Figures 8 and 9 show the variation of WTGS active-power generation against mechanical power input. It can be seen that with the increase of mechanical power input, the WTGS active-power generation also increases linearly.
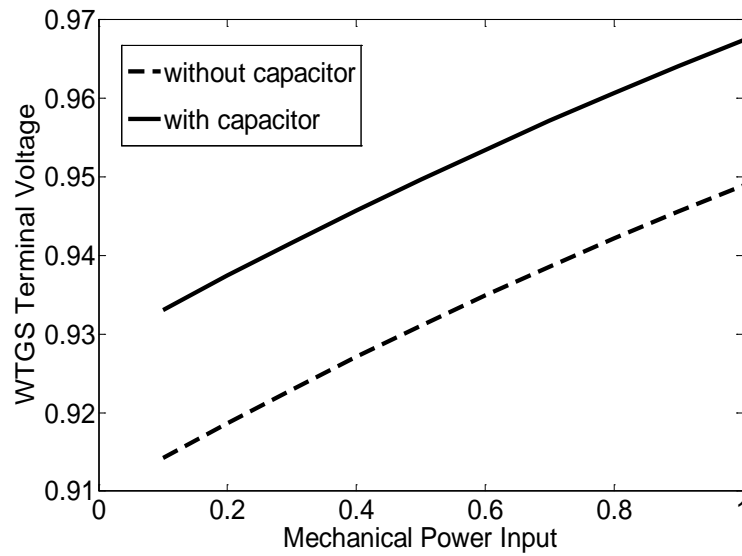
Fig. 6. Variation of WTGS terminal voltage (33-bus).
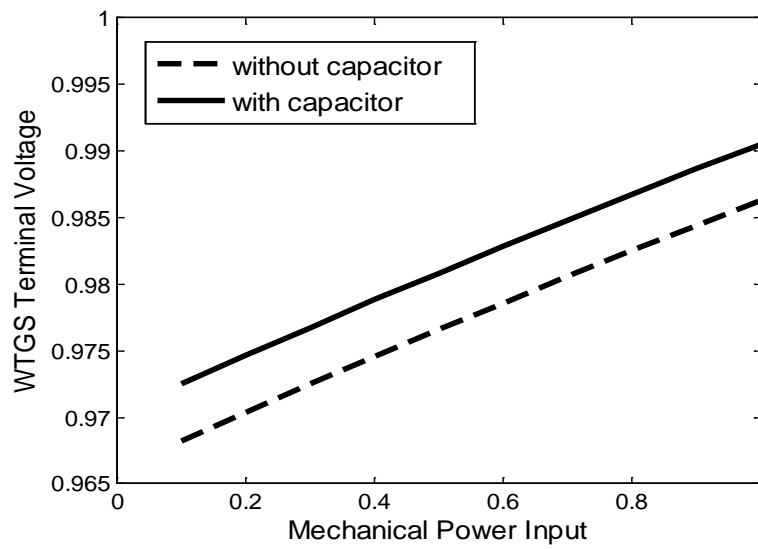
Fig. 7. Variation of WTGS terminal voltage (69-bus).
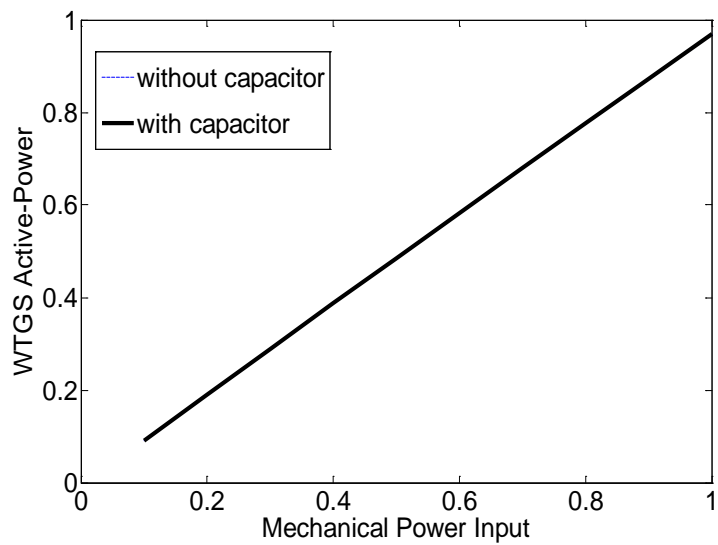
Fig. 8. Variation of WTGS active-power (33-bus).
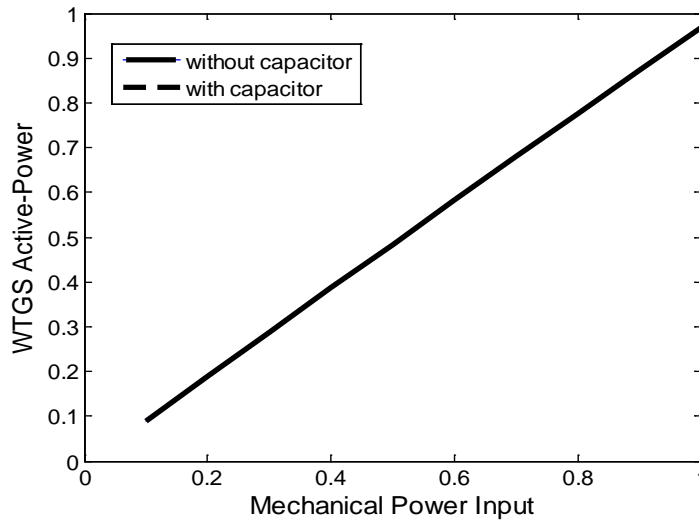
Fig. 9. Variation of WTGS active-power (69-bus).

Variation of WTGS reactive-power generation against mechanical power input is given in Figures 10 and 11. The figures show that the WTGS reactive-power generation increases in a more rapid manner than the increase of mechanical power input. This rapid increase is due to the fact that with higher mechanical power input *(i.e.* higher active-power generation), more reactive-power is consumed by the asynchronous generator of WTGS.
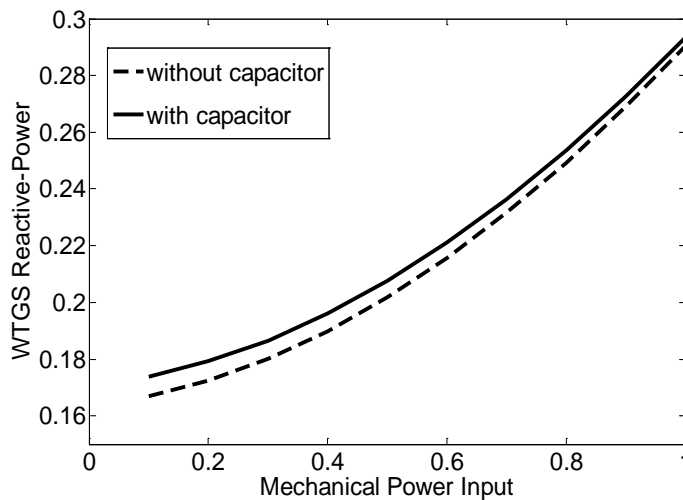
Fig. 10. Variation of WTGS reactive-power (33-bus).
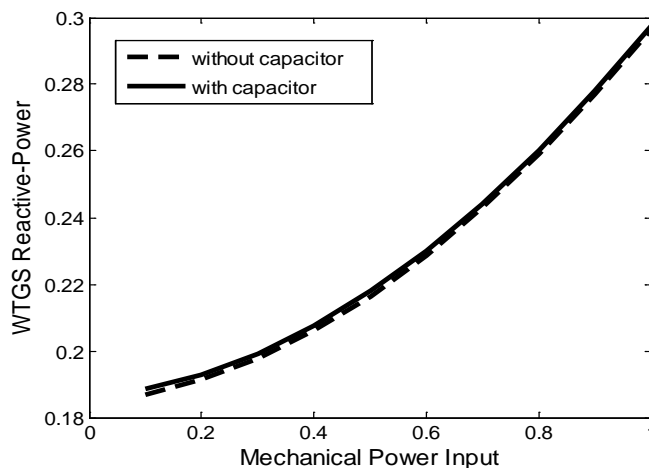
Fig. 11. Variation of WTGS reactive-power (69-bus).

3. CONCLUSION

In the present paper, a simple method for modeling and incorporating fixed-speed WTGS into distribution system load flow analysis has been proposed. The proposed model is developed based on the equivalent T-circuit of the asynchronous machine. It is derived using basic electric circuit theory, where only Kirchhoff and Ohm laws are used in forming the mathematical model. Unlike the previous model (i.e. PQ model), conversion from T-circuit to π-circuit is not necessary in the model derivation process. Moreover, since only one set of equations is needed to represent the WTGS, it is therefore much simpler than the PQ model. The developed mathematical model is then integrated into the distribution system load flow analysis to evaluate steady state operation of the whole system, including the wind turbine system.

It has been shown in the validation study that results from the proposed method are in exact agreement with those from PQ model. For example, for 33-bus system and $P_m = 0.5$ pu, the WTGS terminal voltage is 0.93108 when calculated using the proposed method. The same exact value is obtained when PQ model is used. Therefore, it is confirmed that the proposed T-circuit model is valid and accurate. However, as mentioned before, the proposed method is only applicable for fixed-speed WTGS. For future work, the WTGS model established in the present paper will provide a starting point for further research in modeling and incorporating variable-speed WTGS into power system load flow analysis.

REFERENCES

[1]   Castro L.M., Fuerte-Esquivel C.R., and Tovar-Hernandez J.H., 2011. A Unified approach for the solution of power flows in electric power systems including wind farms. *Electric Power Systems Research* 81: 1859-1865.

[2]   Feijoo A., Pazos J.L and Villanueva D., 2013. Conventional asynchronous wind turbine models – mathematical expressions for the load flow analysis. *International Journal of Energy Engineering (IJEE)* 3(6): 269-278.

[3]   Feijoo A. and D. Villanueva. 2016. A PQ Model for asynchronous machines based on rotor voltage calculation. *IEEE Transaction on Energy Conversion* 2: 813-814.

[4]   Feijoo A. and D. Villanueva. 2016. Correction to 'A PQ model for asynchronous machines based on rotor voltage calculation'. *IEEE Transaction on Energy Conversion* 31(3): 1228-1228.

[5]   Muruganantham B. and R. Gnanadass. 2017. Wind integrated time series load flow analysis for a practical distribution system. *Revista Facultad de Ingenieria* 85: 33-39.

[6]   Ozturk O., Balci M.E. and Hocaoglu M.H., 2018. A new wind turbine generating system model for balanced and unbalanced distribution systems load flow analysis. *Applied Sciences* 8(4): 502-518.

[7]   Haque M.H., 2014. Evaluation of power flow solutions with fixed speed wind turbine generating systems. *Energy Conversion and Management* 79: 511-518.

[8]   Wang J., Huang C. and Zobaa A.F., 2015. Multiple-node models of asynchronous wind turbines in wind farms for load flow analysis. *Electric Power Components and Systems* 44(2): 135-141.

[9]   Haque M.H., 2015. Incorporation of fixed speed wind turbine generators in load flow analysis of distribution systems. *International Journal of Renewable Energy Technology* 6(4): 317-324.

[10] Gianto R., and K.H. Khwee. 2016. A new method for load flow solution of electric power distribution system. *International Review of Electrical Engineering* 11(5): 535-541.

APPENDIX

This section discusses the calculation of the Jacobian matrix using numerical method. The following is the formulation to calculate the Jacobian matrix $\mathbf{J}(\mathbf{x})$ of a vector function $\mathbf{F}(\mathbf{x})$ at the point $\mathbf{x}^*$:

$$\mathbf{J}(\mathbf{x}^*) = \begin{bmatrix} \dfrac{\partial f_1}{\partial x_1} & \dfrac{\partial f_1}{\partial x_2} & \cdots & \dfrac{\partial f_1}{\partial x_n} \\ \dfrac{\partial f_2}{\partial x_1} & \dfrac{\partial f_2}{\partial x_2} & \cdots & \dfrac{\partial f_2}{\partial x_n} \\ \vdots & \vdots & \ddots & \vdots \\ \dfrac{\partial f_n}{\partial x_1} & \dfrac{\partial f_n}{\partial x_2} & \cdots & \dfrac{\partial f_n}{\partial x_n} \end{bmatrix}$$

Elements of $\mathbf{J}(\mathbf{x}^*)$ are computed as the following.

First row:

$$\frac{\partial}{\partial x_1} f_1(\mathbf{x}^*) \approx \frac{f_1(x_1^* + h, x_2^*, x_3^*, \ldots, x_n^*) - f_1(x_1^* - h, x_2^*, x_3^*, \ldots, x_n^*)}{2h}$$

$$\frac{\partial}{\partial x_2} f_1(\mathbf{x}^*) \approx \frac{f_1(x_1^*, x_2^* + h, x_3^*, \ldots, x_n^*) - f_1(x_1^*, x_2^* - h, x_3^*, \ldots, x_n^*)}{2h}$$

$$\vdots$$

$$\frac{\partial}{\partial x_n} f_1(\mathbf{x}^*) \approx \frac{f_1(x_1^*, x_2^*, x_3^*, \ldots, x_n^* + h) - f_1(x_1^*, x_2^*, x_3^*, \ldots, x_n^* - h)}{2h}$$

Second row:

$$\frac{\partial}{\partial x_1} f_2(\mathbf{x}^*) \approx \frac{f_2(x_1^* + h, x_2^*, x_3^*, \ldots, x_n^*) - f_2(x_1^* - h, x_2^*, x_3^*, \ldots, x_n^*)}{2h}$$

$$\frac{\partial}{\partial x_2} f_2(\mathbf{x}^*) \approx \frac{f_2(x_1^*, x_2^* + h, x_3^*, \ldots, x_n^*) - f_2(x_1^*, x_2^* - h, x_3^*, \ldots, x_n^*)}{2h}$$

$$\vdots$$
$$\vdots$$

$$\frac{\partial}{\partial x_n} f_2(\mathbf{x}^*) \approx \frac{f_2(x_1^*, x_2^*, x_3^*, \ldots, x_n^* + h) - f_2(x_1^*, x_2^*, x_3^*, \ldots, x_n^* - h)}{2h}$$

n^{th} row:

$$\frac{\partial}{\partial x_1} f_n(\mathbf{x}^*) \approx \frac{f_n(x_1^* + h, x_2^*, x_3^*, \ldots, x_n^*) - f_n(x_1^* - h, x_2^*, x_3^*, \ldots, x_n^*)}{2h}$$

$$\frac{\partial}{\partial x_2} f_n(\mathbf{x}^*) \approx \frac{f_n(x_1^*, x_2^* + h, x_3^*, \ldots, x_n^*) - f_n(x_1^*, x_2^* - h, x_3^*, \ldots, x_n^*)}{2h}$$

$$\vdots$$
$$\vdots$$

$$\frac{\partial}{\partial x_n} f_n(\mathbf{x}^*) \approx \frac{f_n(x_1^*, x_2^*, x_3^*, \ldots, x_n^* + h) - f_n(x_1^*, x_2^*, x_3^*, \ldots, x_n^* - h)}{2h}$$

In the above formulas, h is a constant and has a small numerical value (for example: 0.01; 0.001; or 0.0001).